M. Rivers and A. Tkachenko for discussions, and D. Stockwell for the donation of mustard seeds for the experiment. G.F.D. acknowledges a postdoctoral Grainger Fellowship. This work was supported by an NSF research grant and by the MRSEC program of the NSF.

Correspondence and requests for materials should be addressed to H.M.J. (e-mail: h-jaeger@uchicago.edu).

Oscillatory cluster patterns in a homogeneous chemical system with global feedback

Vladimir K. Vanag, Lingfa Yang, Milos Dolnik, Anatol M. Zhabotinsky & Irving R. Epstein

Department of Chemistry and Volen Center for Complex Systems, MS 015, Brandeis University, Waltham, Massachusetts 02454-9110, USA

Oscillatory clusters are sets of domains in which nearly all elements in a given domain oscillate with the same amplitude and phase[1–4]. They play an important role in understanding coupled neuron systems[5–8]. In the simplest case, a system consists of two clusters that oscillate in antiphase and can each occupy multiple fixed spatial domains. Examples of cluster behaviour in extended chemical systems are rare, but have been shown to resemble standing waves[9–13], except that they lack a characteristic wavelength. Here we report the observation of so-called 'localized clusters'—periodic antiphase oscillations in one part of the medium, while the remainder appears uniform—in the Belousov–Zhabotinsky reaction–diffusion system with photochemical global feedback. We also observe standing clusters with fixed spatial domains that oscillate periodically in time and occupy the entire medium, and irregular clusters with no periodicity in either space or time, with standing clusters transforming into irregular clusters and then into localized clusters as the strength of the global negative feedback is gradually increased. By incorporating the effects of global feedback into a model of the reaction, we are able to simulate successfully the experimental data.

The Belousov–Zhabotinsky (BZ) reaction is the best studied chemical oscillator; its dynamics resemble those of many important biological and physical nonlinear oscillators[14–19]. The reaction consists of the oxidation of malonic acid by bromate, catalysed by metal ions or metallo-complexes in acidic aqueous solution.

Here we study pattern formation in the photosensitive $Ru(bpy)_3$-catalysed BZ reaction[20–22] in a thin layer of silica gel[23,24] with photochemical global negative feedback imposed through illumination (see Fig. 1). The average concentration of $Ru(bpy)_3^{3+}$, Z_{av}, taken over the working area of the gel, is employed to control the intensity I of actinic light (from lamp L2), according to $I = I_{max}\sin^2(g(Z_{av} - Z_t))$, where g is the feedback coefficient and Z_t is a target concentration. The target Z_t is varied by changing the reference voltage (RV) and is set close to the steady state value, Z_{ss}, in such a way that the difference $Z_{av} - Z_t$ is always positive. The angle between polarizers P1 and P2 (that is, $g(Z_{av} - Z_t)$) is not allowed to exceed $\pi/2$. The gain of amplifier A5 is used to control the feedback coefficient g. The actinic light produces bromide ion[21], which inhibits the oxidation of $Ru(bpy)_3^{2+}$.

We investigate how pattern formation depends on g. We choose the initial reagent concentrations in such a way that without any feedback the system generates bulk oscillations. Various travelling wave patterns are found when g is less than $g^\star$, a value that depends on the initial concentrations of reagents. In most cases, $1 \times 10^4\,M^{-1} < g^\star < 2 \times 10^4\,M^{-1}$. When the feedback coefficient is slightly above $g^\star$, either travelling wave patterns or cluster patterns are observed, depending on the initial conditions. The width of this bistability range depends on the initial reagent concentrations.

When g exceeds $2 \times 10^4\,M^{-1}$, standing clusters arise. Figure 2 depicts several patterns of such clusters. Figure 2a shows one period of oscillation of a pattern that arose from initial conditions created by brief illumination of the gel through a striped mask. At $t = 4$ s, Z_{av} reaches a maximum. After this instant, the white domains start to fade and the system gradually evolves to the uniform reduced (dark) state. During the second half-period, the regions that were dark during the first half-period become bright, and at $t = 29$ s the pattern displays another maximum in Z_{av}. As adjacent domains oscillate in antiphase, the period, T_{av}, of oscillations of Z_{av} is half the period of the local oscillations. Figures 2b and 2c show patterns that developed from a spiral wave and from uniform initial conditions, respectively. Other patterns of standing clusters can be obtained by varying the initial conditions. Standing clusters do not possess intrinsic spatial periodicity, because the global feedback is sensitive only to the spatially integrated characteristics of the patterns.

At larger g, two other types of patterns arise. If the initial reagent concentrations lie far from the boundary of the oscillatory region of the parameter space, we observe a transition from standing clusters

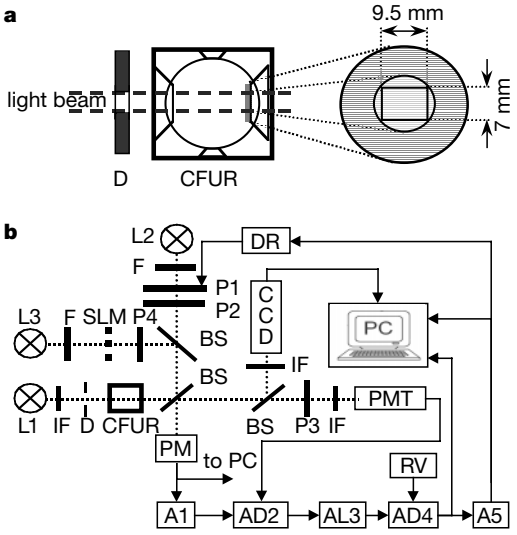

Figure 1 Experimental set-up. **a**, The continuously fed unstirred reactor (CFUR) consists of a 24-ml continuously stirred tank reactor thermostated at 25 °C and a thin layer of silica gel polymerized on the reactor optical window (grey circle). The 0.413-mm-thick gel has diameter 22 mm, and contains 1.5 mM of immobilized Tris(2,2′-bipyridyl)ruthenium(II)($Ru(bpy)_3^{2+}$. Diaphragm D selects an illuminated working area of gel (light grey circle). The rectangular frame shows the field of view of the CCD camera. A peristaltic pump injects stock solutions of KBr, malonic acid, $NaBrO_3$ and H_2SO_4 into a premixing chamber (not shown) and then into the CFUR. **b**, Low-intensity analysing light from the stabilized 45-W light source (L1) passes through the working area of the gel, and is collected by a lens and directed to the photomultiplier tube (PMT). AD2 and AD4 are differential amplifiers, AL3 is a logarithmic amplifier, A5 is a d.c. amplifier. The driver (DR) rotates polarizer P1, and controls the intensity of actinic light from the 450-W Xe arc lamp (L2). P1–P4 are polarizers, IFs are interference filters with $\lambda_{max} = 450$ nm, Fs are bandpass filters (400–500 nm), BSs are beam splitters; lenses and collimators are not shown. The 150-W Xe arc lamp (L3) serves to set patterns of initial conditions. An image of the spatial light modulator (SLM) is focused in the plane of the silica gel. Actinic light intensity (I) is measured by the power meter (PM). Polarizers P2-P3 and P4-P3 are crossed to separate optical channels. The remaining parasitic signal from scattered actinic light is compensated electronically by amplifiers A1 and AD2, and stays below 1% of the photomultiplier working signal when I varies from 0 to $I_{max} = 4.3\,mW\,cm^{-2}$. Uniformity of illumination of the working area is better than 2%.

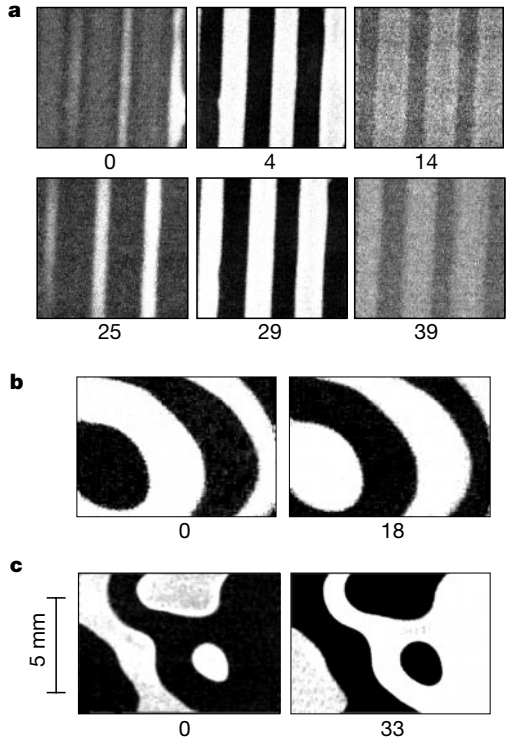

Figure 2 Standing clusters. **a**, One period of oscillation of the pattern formed by initial constant illumination through a striped mask. **b**, The pattern that evolves from an initial spiral wave. Snapshots are taken at two consecutive moments of maximum Z_{av}. **c**, Standing clusters obtained from uniform initial conditions—the gel area was illuminated with constant light to suppress pattern formation, then feedback was switched on and simultaneously constant illumination was switched off. Grey levels quantify $[Ru(bpy)_3^{3+}]$, with white corresponding to maximum and black to minimum. Numbers under frames show time in seconds starting from the beginning (maximum or minimum Z_{av}) of an arbitrary cycle in the stationary regime. Initial reagent concentrations (M) and feedback coefficient (M^{-1}) are: **a**, $[H_2SO_4]_0 = 0.7$, $[BrO_3^-]_0 = 0.28$, $[MA]_0 = 0.2$, $[Br^-]_0 = 0.125$, $g = 2.7 \times 10^4$; **b**, $[H_2SO_4]_0 = 0.7$, $[BrO_3^-]_0 = 0.4$, $[MA]_0 = 0.2$, $[Br^-]_0 = 0.125$, $g = 5.5 \times 10^4$; **c**, $[H_2SO_4]_0 = 0.5$, $[BrO_3^-]_0 = 0.25$, $[MA]_0 = 0.3$, $[Br^-]_0 = 0.1$, $g = 5.5 \times 10^4$. Residence time of fluid in the CSTR is 1,000 s.

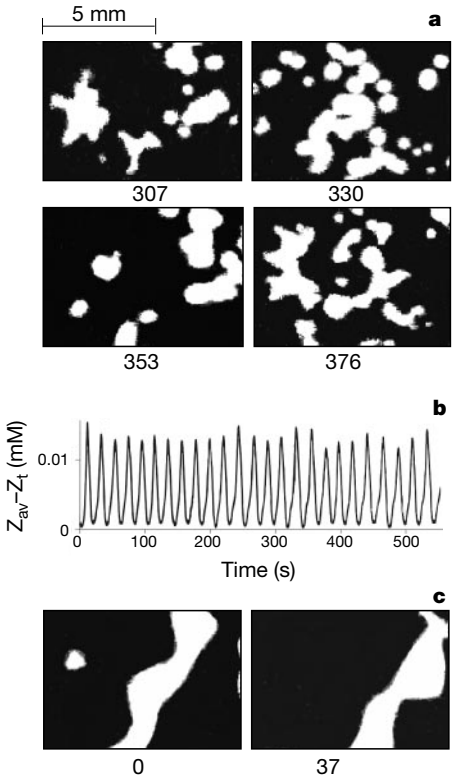

Figure 3 Irregular and localized clusters. Snapshots are taken at consecutive maxima of average concentration of $Ru(bpy)_3^{3+}$ (Z_{av}). **a**, Irregular clusters. Initial concentrations (M): $[H_2SO_4]_0 = 0.75$, $[BrO_3^-]_0 = 0.312$, $[MA]_0 = 0.375$, $[Br^-]_0 = 0.125$, residence time is 667 s; $g = 1.5 \times 10^5\ M^{-1}$. **b**, Oscillations of Z_{av} corresponding to **a**. **c**, Localized clusters. Initial concentrations (M): $[H_2SO_4]_0 = 0.5$, $[BrO_3^-]_0 = 0.25$, $[MA]_0 = 0.3$, $[Br^-]_0 = 0.1$ (same as in Fig. 2c); residence time is 1,000 s; $g = 2.2 \times 10^5\ M^{-1}$. Other conditions as in Fig. 2.

to a phenomenon we dub irregular clusters. Local oscillations in these patterns are aperiodic, but the average concentration, Z_{av}, (and, consequently, I) oscillates approximately periodically, and the period, T_{av}, provides a convenient scale for analysing the dynamics of irregular clusters (see Fig. 3b). Figure 3a displays snapshots of irregular clusters separated by T_{av}. Using image analysis techniques we compare the locations of the white domains at successive maxima of Z_{av}. We find that the white domains of two consecutive patterns do not overlap, which indicates antiphase oscillations. The overlapping area of white domains in frames separated by $2T_{av}$ is relatively small, which demonstrates the absence of temporal periodicity. Over a full standing cluster cycle ($2T_{av}$), the white domains of antiphase oscillations cover the entire area of the system. In an irregular cluster, only part of the medium is occupied by the white domains of two consecutive patterns over $2T_{av}$. Because the irregular cluster patterns are not stationary, the entire area is eventually covered by the white domains, typically over several tens of periods.

Localized clusters arise if the initial reagent concentrations are close to the parameter-space boundary between the oscillatory and the reduced steady-state regions. Domains of antiphase oscillations in localized clusters occupy only part of the area, while no pattern can be seen in the remaining part of the system. In Fig. 3c, two snapshots separated by half a period of oscillations show two adjacent large domains of antiphase oscillations separated by a nodal line. In the first snapshot ($t = 0$), there are also two small domains at the right boundary of the frame and one small domain not far from the left boundary. The latter domain is within the area with no visible pattern.

With increasing feedback coefficient, the portion of the medium occupied by clusters shrinks. Eventually, clusters disappear, giving way to small-amplitude bulk oscillations. This transition takes place in the range $2 \times 10^5\ M^{-1} < g < 3.5 \times 10^5\ M^{-1}$, depending on the initial reagent concentrations.

To simulate the pattern formation observed in our experiments, we employ a model of the BZ reaction[25,26] with the rate constants adjusted according to ref. 27. We add a global linear feedback term to account for the bromide ion production that results from the actinic illumination, $v_{GF} = g\varphi I_{max}(Z_{av} - Z_{ss})$, where φ is the quantum yield. The results of our simulations mimic those of the experiments. Bulk oscillations and travelling waves are observed in the model for smaller values of g. Spontaneous formation of spiral waves predominates at low g. Standing clusters emerge for larger values of the feedback coefficient. Depending on the distance from the boundary between the oscillatory and reduced steady-state parameter regions, we obtain sequences of standing, irregular and localized clusters as shown in Fig. 4 (parameters close to the Hopf bifurcation line) or standing and irregular clusters only (parameters further from the Hopf line). In the simulations, standing clusters arise at lower values of g, irregular clusters at intermediate g, localized clusters at larger g, and small-amplitude bulk oscillations at the largest g, as in the experiments. We also performed simulations with the nonlinear feedback term employed in the experiments and obtained qualitatively the same results. The only

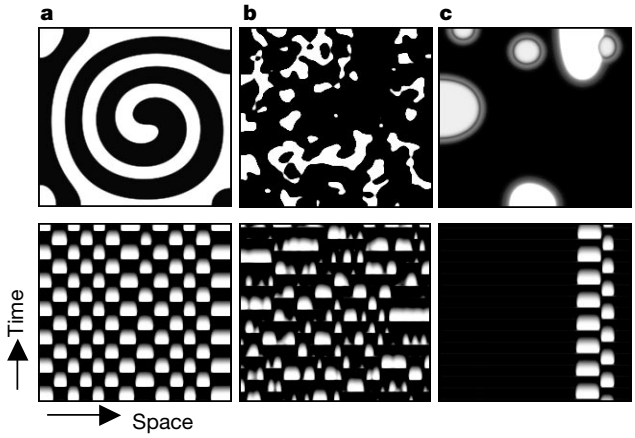

Figure 4 Oscillatory cluster patterns in our BZ reaction–diffusion model with global negative feedback. **a**, Standing clusters: $g = 2 \times 10^4\,M^{-1}$. **b**, Irregular clusters: $g = 5 \times 10^4\,M^{-1}$. **c**, Localized clusters: $g = 1.1 \times 10^5\,M^{-1}$. Top frames display snapshots of patterns; bottom frames show spatio-temporal behaviour along bottom left–top right diagonal of corresponding squares during 380 s. System size is $1 \times 1\,cm^2$ (200×200 grid points). The initial condition for standing clusters is a spiral wave. Irregular and localized clusters are obtained from the pattern shown in **a** by instantaneous increase of feedback coefficient. Simulation is based on a two-variable model: $\partial X/\partial t = (-k_2X + k_3A)/(k_2X + k_3A)\{qk_7k_8BZ/[k_8 + k_{-7}h_0(C-Z)] + k_9B + v_{GF}\} - 2k_4X^2 + k_5h_0AX - k_{-5}U^2 + D_X\partial^2X/\partial r^2$, $\partial Z/\partial t = k_6U(C-Z) - k_{-6}XZ - k_7k_8BZ/[k_8 + k_{-7}h_0(C-Z)] + D_Z\partial^2Z/\partial r^2$, where $U = -k_6(C-Z)/(4k_{-5}) + \{[k_6(C-Z)]^2 + 8k_{-5}X(2k_5h_0A + k_{-6}Z)\}^{1/2}/(4k_{-5})$. Here X, Z, U, A and B are concentrations of $HBrO_2$, $Ru(bpy)_3^{3+}$, $HBrO_2^+$, $HBrO_3$ and malonic acid, respectively. C is the total concentration of catalyst, $[Ru(bpy)_3^{3+}] + [Ru(bpy)_3^{2+}]$, h_0 is the Hammett acidity function, and D_X, and D_Z are diffusion coefficients. v_{GF} is the global feedback term. Rate constants and parameters are: $k_2 = 2.0 \times 10^6\,M^{-2}\,s^{-1}$, $k_3 = 2M^{-2}\,s^{-1}$, $k_4 = 3 \times 10^3\,M^{-1}\,s^{-1}$, $k_5 = 33\,M^{-2}\,s^{-1}$, $k_{-5} = 4.2 \times 10^6\,M^{-1}\,s^{-1}$, $k_6 = 4.0 \times 10^6\,M^{-1}\,s^{-1}$, $k_{-6} = 3.0 \times 10^2\,M^{-1}\,s^{-1}$, $k_7 = 9.2 \times 10^{-1}\,M^{-1}\,s^{-1}$, $k_8/k_{-7} = 2.5 \times 10^{-4}\,M^2$, $k_9 = 3.0 \times 10^{-6}\,s^{-1}$, $A = 0.278\,M$, $B = 0.45\,M$, $C = 2.0 \times 10^{-3}\,M$, $h_0 = 0.25\,M$, $q = 0.7$, $D_X = 1.5 \times 10^{-5}\,cm^2\,s^{-1}$, $D_Z = 2.0 \times 10^{-6}\,cm^2\,s^{-1}$ and $\varphi I_{max} = 1 \times 10^{-5}\,M\,s^{-1}$.

exception was that we found only transient localized clusters, which maintained their positions for just a few periods of oscillation.

Time–space plots of the one-dimensional sections of the system in Fig. 4 clarify the dynamics of the system. Irregular clusters are aperiodic in time on a scale at least an order of magnitude larger than the period of oscillation of standing or localized clusters. Our simulations also reveal that the region of travelling wave patterns often overlaps with a part of the standing cluster region, forming a region of bistability on the g-axis, as found in the experiments. The simulations show that diffusion determines a minimum linear size for the domains and a maximum curvature for the nodal lines.

As the global negative feedback gradually increases, the following sequence of patterns is found in our experiments and simulations: bulk oscillations, wave patterns, standing clusters, irregular clusters, localized clusters, small-amplitude bulk oscillations. We suggest that this sequence is fundamental and will be found in other chemical and biological extended systems with global coupling. The discovery of localized clusters is of particular significance, because an enormous variety of patterns of this type can be created from different initial conditions, and their localized character makes them more convenient for information storage and retrieval than patterns that occupy the entire system. Thus they appear to be well suited for natural systems of distributed memory. Cluster formation in models of neural networks with negative global coupling has received considerable attention[5,7,8], but the experimental observation of such patterns is difficult. We hope that our findings will stimulate a search for analogous dynamic patterns in natural neural systems. □

Received 11 January; accepted 22 May 2000.

1. Golomb, D., Hansel, D., Shraiman, B. & Sompolinsky, H. Clustering in globally coupled phase oscillators. *Phys. Rev. A* **45,** 3516–3530 (1992).
2. Hakim, V. & Rappel, W.-J. Dynamics of the globally coupled complex Ginzburg-Landau equation. *Phys. Rev. A* **46,** 7347–7350 (1992).
3. Falcke, M., Engel, H. & Neufeld, M. Cluster formation, standing waves, and stripe patterns in oscillatory active media with local and global coupling. *Phys. Rev. E* **52,** 763–771 (1995).
4. Wang, W., Kiss, I. Z. & Hudson, J. L. Experiments on arrays of globally coupled chaotic electrochemical oscillators: Synchronization and clustering. *Chaos* **10,** 248–256 (2000).
5. Golomb, D. & Rinzel, J. Clustering in globally coupled inhibitory neurons. *Physica D* **72,** 259–282 (1994).
6. Terman, D. & Wang, D. Global competition and local cooperation in a network of neural oscillators. *Physica D* **81,** 148–176 (1995).
7. Huerta, R., Bazhenov, M. & Rabinovich, M. I. Clusters of synchronization and bistability in lattices of chaotic neurons. *Europhys. Lett.* **43,** 719–724 (1998).
8. Rabinovich, M. I., Varona, P. & Torres, J. J. Slow dynamics and regularization phenomena in ensembles of chaotic neurons. *Physica A* **263,** 405–414 (1999).
9. Lev, O., Sheintuch, M., Pismen, L. M. & Yarnitzky, Ch. Standing and propagating wave oscillations in the anodic dissolution of nickel. *Nature* **336,** 458–459 (1988).
10. Cordonier, G. A., Schuth, F. & Schmidt, L. D. Oscillations in methylamine decomposition on Pt, Rh, and Ir: Experiments and models. *J. Chem. Phys.* **91,** 5374–5386 (1989).
11. Jakubith, S., Rotermund, H. H., Engel, W., von Oertzen, A. & Ertl, G. Spatiotemporal concentration patterns in a surface reaction: Propagating and standing waves, rotating spirals, and turbulence. *Phys. Rev. Lett.* **65,** 3013–3016 (1990).
12. Somani, M., Liauw, M. A. & Luss, D. Evolution and impact of temperature patterns during hydrogen oxidation on a Ni ring. *Chem. Eng. Sci.* **52,** 2331–2341 (1997).
13. Petrov, V., Ouyang, Q. & Swinney, H. L. Resonant pattern formation in a chemical system. *Nature* **388,** 655–657 (1997).
14. Belousov, B. P. in *Collection of Short Papers on Radiation Medicine* 145–152 (Medgiz, Moscow, 1959).
15. Zhabotinsky, A. M. Periodic liquid phase reactions. *Proc. Acad. Sci. USSR* **157,** 392–395 (1964).
16. Zaikin, A. N. & Zhabotinsky, A. M. Concentration wave propagation in a two-dimensional, liquid phase self-oscillating system. *Nature* **225,** 535–537 (1970).
17. Winfree, A. T. Spiral waves of chemical activity. *Science* **175,** 634–636 (1972).
18. Ross, J., Müller, S. C. & Vidal, C. Chemical waves. *Science* **240,** 460–465 (1988).
19. Kapral, R. & Showalter, K. (eds) *Chemical Waves and Patterns* (Kluwer, Dordrecht, 1995).
20. Kuhnert, L., Agladze, K. I. & Krinsky, V. I. Image processing using light-sensitive chemical waves. *Nature* **337,** 244–247 (1989).
21. Grill, S., Zykov, V. S. & Müller, S. C. Feedback-controlled dynamics of meandering spiral waves. *Phys. Rev. Lett.* **75,** 3368–3371 (1995).
22. Kadar, S., Amemiya, T. & Showalter, K. Reaction mechanism for light sensitivity of the $Ru(bpy)_3^{2+}$-catalyzed Belousov-Zhabotinsky reaction. *J. Phys. Chem. A* **101,** 8200–8206 (1997).
23. Yamaguchi, T., Kuhnert, L., Nagy-Ungvarai, Zs., Müller, S. C. & Hess, B. Gel systems for the Belousov-Zhabotinskii reaction. *J. Chem. Phys.* **95,** 5831–5837 (1991).
24. Amemiya, T., Kettunen, P., Kadar, S., Yamaguchi, T. & Showalter, K. Formation and evolution of scroll waves in photosensitive excitable media. *Chaos* **8,** 872–878 (1998).
25. Zhabotinsky, A. M., Buchholtz, F., Kiyatkin, A. B. & Epstein, I. R. Oscillations and waves in metal-ion-catalyzed bromate oscillating reactions in highly oxidized states. *J. Phys. Chem.* **97,** 7578–7584 (1993).
26. Bugrim, A., Dolnik, M., Zhabotinsky, A. M. & Epstein, I. R. Heterogeneous sources of target patterns in reaction-diffusion systems. *J. Phys. Chem.* **100,** 19017–19022 (1996).
27. Gao, Y. & Försterling, H.-D. Oscillations in the bromomalonic acid/bromate system catalyzed by $[Ru(bipy)_3]^{2+}$. *J. Phys. Chem.* **99,** 8638–8644 (1995).

Acknowledgements

This work was supported by the Chemistry Division of the National Science Foundation and the W. M. Keck Foundation.

Correspondence and requests for materials should be addressed to A.M.Z. (e-mail: zhabotinsky@brandeis.edu)